

New Numerical Treatment for the Generalized Regularized Long Wave Equation Based on Finite Difference Scheme

Talaat S. EL-Danaf, K. R. Raslan, Khalid K. Ali

Abstract-In this paper, the generalized regularized long wave (GRLW) equation is solved numerically using the finite difference method. Fourier stability analysis of the linearized scheme shows that it is unconditionally stable. Also, the local truncation error of the method is investigated. Three invariants of motion are evaluated to determine the conservation properties of the problem, and the numerical scheme leads to accurate and efficient results. Moreover, interaction of two and three solitary waves is shown. The development of the Maxwellian initial condition into solitary waves is also shown and we show that the number of solitons which are generated from the Maxwellian initial condition can be determined. Numerical results show also that a tail of small amplitude appears after the interactions.

Keywords: Finite difference; generalized Regularized long wave equation; Solitary waves; Solitons.

I. INTRODUCTION

The regularized long wave (RLW) equation of the form

$$u_t + u_x + \varepsilon uu_x - \mu u_{xxt} = 0, \quad (1)$$

where ε and μ are positive constants, was originally introduced to describe the behavior of the undular bore by Peregrine [1]. This equation is very important in physics media since it describes phenomena with weak nonlinearity and dispersion waves, including nonlinear transverse waves in shallow water, ion-acoustic and magneto hydrodynamic waves in plasma and phonon packets in nonlinear crystals. In previous work [1-15], the RLW equation is solved by various methods such as finite difference methods, finite element methods including collocation method with quadratic B-splines, cubic B-splines and recently septic splines. The modified regularized long wave (MRLW) equation of the form

$$u_t + u_x + \varepsilon u^2 u_x - \mu u_{xxt} = 0, \quad (2)$$

was considered by Gardner used B-spline finite element [16], Khalifa et al, used finite difference methods [17], Raslan and Hassan used Solitary waves for the MRLW equation [18], Khalifa et al, used collocation methods with quadratic B-splines and cubic B-splines [19], recently Hassan and Alamery used quintic B-splines and Sextic B-splines [20], methods. Indeed the RLW and MRLW equations are special cases of the generalized long wave (GRLW) equation which has the form

$$u_t + u_x + p(p+1)u^p u_x - \mu u_{xxt} = 0, \quad (3)$$

where μ is positive constants and p is a positive integer. The GRLW equation is studied by few authors, Mokhtari used Sinc-collocation [21], Kaya used a numerical simulation of solitary wave solutions [22], El-Danaf et al, used Adomian decomposition method (ADM) [23] and Thoudam Roshan used a petrov-Galerkin method [25], Mohammadi used the basis of a reproducing kernel space [26]. The purpose of this paper is to present a conservative finite difference scheme for the (GRLW) (3). Fourier stability analysis of the linearized scheme shows that it is unconditionally stable. Also, the local truncation error of the method is investigated. The interaction of solitary waves and other properties of the GRLW equation are studied.

II. THE PROBLEM AND ANALYTICAL SOLUTION

The GRLW (3) we can write it in this form [25]

$$u_t + u_x + \varepsilon u^p u_x - \mu u_{xxt} = 0, \quad (4)$$

where $\varepsilon = p(p+1)$ and subscripts x and t denote differentiation, is considered with the boundary conditions $u \rightarrow 0$ as $x \rightarrow \pm\infty$. In this work, periodic boundary conditions on the region $a \leq x \leq b$ are assumed in the form:

$$\begin{aligned} u(a,t) = u(b,t) = 0, \quad u_x(a,t) = u_x(b,t) = 0, \\ u_{xx}(a,t) = u_{xx}(b,t) = 0, \end{aligned} \quad (5)$$

and then the analytical solutions of (3) take the form.[25]

$$u(x,t) = p \sqrt{\frac{(p+2)c}{2p}} \operatorname{sech} \left(\frac{p}{2} \sqrt{\frac{c}{\mu(c+1)}} (x - (c+1)t - x_0) \right), \quad (6)$$

where x_0 is an arbitrary constant. Actually it is not always available to get an analytic solution for nonlinear partial differential equations, so we try to provide numerical methods to solve such problems.

III. CONSERVATION LAWS AND L_2, L_∞ FOR THE GRLW EQUATION

The numerical solutions of the GRLW equation must preserve the conservation laws during propagation as discuss the three invariant conditions which correspond to the conservation of mass, momentum and energy [25] respectively.

$$I_1 = \int_a^b u \, dx, \quad I_2 = \int_a^b (u^2 + u_x^2) \, dx, \quad I_3 = \int_a^b (u^4 - u_x^2) \, dx, \quad (7)$$

The accuracy of the method is measured using the following error norms

Manuscript Received on September 2014.

Talaat S. EL-Danaf, Department of Mathematics, Faculty of Science, Menoufia University, Shebein El-Koom, Egypt.

K. R. Raslan, Department of Mathematics, Faculty of Science, Al-Azhar University, Nasr-City, Cairo, Egypt.

Khalid K. Ali, Department of Mathematics, Faculty of Science, Al-Azhar University, Nasr-City, Cairo, Egypt..

$$L_2 = \|u^E - u^N\| = \sqrt{h \sum_{j=0}^N (u_j^E - u_j^N)^2}, \quad (8)$$

$$L_\infty = \max_j |u_j^E - u_j^N|, \quad (9)$$

IV. FINITE DIFFRENECE SCHEMES FOR THE GRLW EQUATION

We solve the GRLW equation by using finite difference methods. We discuss three finite difference schemes for the GRLW (4).

4.1- A weighted average approximation (1st scheme) - stability and error analysis

To apply the finite difference method for solving the GRLW equation, firstly we present the following notations for the derivatives

$$\begin{aligned} \frac{\partial u(x_j, t_n)}{\partial t} &\equiv (u_t)_j^n \equiv \frac{u_j^{n+1} - u_j^n}{k}, \\ ((1 + \varepsilon u^p)u_x)_j^n &\equiv \theta(1 + \varepsilon(u_{j-1}^n)^p) \frac{u_{j+1}^{n+1} - u_{j-1}^{n+1}}{2h} + \\ &\quad (1 - \theta)(1 + \varepsilon(u_j^n)^p) \frac{u_{j+1}^n - u_{j-1}^n}{2h}, \\ (u_{xxt})_j^n &\equiv \frac{(u_{j+1}^{n+1} - 2u_j^{n+1} + u_{j-1}^{n+1}) - (u_{j+1}^n - 2u_j^n + u_{j-1}^n)}{2kh^2}, \end{aligned} \quad (10)$$

where u_j^n is the exact solution at (x_j, t_n) , $0 \leq \theta \leq 1$ and h, k are the spatial and temporal step sizes respectively and, $x_j = jh, t_n = nk$, and $n = 0, 1, \dots$, where superscript n denotes a quantity associated with time level t_n and subscript j denotes a quantity associated with space mesh point x_j .

Now, we assume that u_j^n is the exact solution at the grid point (x_j, t_n) and U_j^n is the approximation solution at the same point. Then the finite difference scheme for the (4) becomes,

$$\begin{aligned} \frac{U_j^{n+1} - U_j^n}{k} + \theta(1 + \varepsilon(U_{j-1}^n)^p) \frac{U_{j+1}^{n+1} - U_{j-1}^{n+1}}{2h} + \\ (1 - \theta)(1 + \varepsilon(U_j^n)^p) \frac{U_{j+1}^n - U_{j-1}^n}{2h} - \\ \mu \frac{(U_{j+1}^{n+1} - 2U_j^{n+1} + U_{j-1}^{n+1}) - (U_{j+1}^n - 2U_j^n + U_{j-1}^n)}{2kh^2} = 0. \end{aligned} \quad (11)$$

Then (11) can be written as,

$$\begin{aligned} (\mu + \theta \frac{kh}{2} (1 + \varepsilon(U_{j-1}^n)^p)) U_{j-1}^{n+1} - (2\mu + h^2) U_j^{n+1} + \\ (\mu - \theta \frac{kh}{2} (1 + \varepsilon(U_{j-1}^n)^p)) U_{j+1}^{n+1} = (\mu - (1 - \theta) \frac{kh}{2} \\ (1 + \varepsilon(U_j^n)^p)) U_{j-1}^n - (2\mu + h^2) U_j^n + \\ (\mu + (1 - \theta) \frac{kh}{2} (1 + \varepsilon(U_j^n)^p)) U_{j+1}^n \end{aligned} \quad (12)$$

4.1.1- Stability of finite difference for (1st scheme)

Lemma(1): The finite difference scheme (12) is unconditional stable and if $u(x, t)$ is smooth enough, then

the local truncation error T_j^n of the scheme (12) is $O(h^2 + k)$.

Proof. Using Fourier method, assuming that u in the nonlinear term is locally constant. In case of applying the Von Neumann stability theory, the growth of Fourier mode takes the form

$$U_j^n = \zeta^n e^{ikx_j}, \quad (13)$$

where k is a mode number, h is the element size and $x_j = jh, i = \sqrt{-1}$ Now, substituting (13) into (12) yields

$$\begin{aligned} g[(\mu + Q\theta)e^{-ikh} - (2\mu + h^2) + (\mu - Q\theta)e^{ikh}] \\ = (\mu - Q)(1 - \theta)e^{-ikh} - (2\mu + h^2) + (\mu + Q)(1 - \theta)e^{ikh}, \end{aligned} \quad (14)$$

where $Q = \frac{kh}{2} (1 + \varepsilon(U_j^n)^p)$, $g = \frac{\zeta^{n+1}}{\zeta^n}$,

then we can get the amplification factor in the form

$$g = \frac{A + i(1 - \theta)B}{A - i\theta B}, \quad (15)$$

where $A = 2\mu \cos kh - (2\mu + h^2)$, $B = 2Q \sin kh$.

Now, we discuss the stability of this scheme

(1) For Crank-Nicholson scheme

Substituting the values of $\theta = 0.5$ into (15) yields

$$g = \frac{A + i\frac{1}{2}B}{A - i\frac{1}{2}B}. \quad (16)$$

Then we get

$$|g| = 1, \quad (17)$$

so we can say that the Crank-Nicholson scheme is unconditional stable.

(2) The fully implicit scheme.

Substituting the values of $\theta = 1$ into (15) yields

$$g = \frac{A}{A - iB}. \quad (18)$$

Then we get

$$|g| < 1, \quad (19)$$

so we can say that the implicit scheme is unconditional stable.

Now, to study the local truncation error of (12) we replace

U_j^n by $v_j^n = u(x_j, t_n)$ represents the analytical solution for the (4) with independent variables x and t and let $p = 3$, (GRLW) equation, then substituting it into (12) gives

$$\begin{aligned} (\mu + \theta \frac{kh}{2} (1 + \varepsilon(v_{j-1}^n)^3)) v_{j-1}^{n+1} - (2\mu + h^2) v_j^{n+1} + \\ (\mu - \theta \frac{kh}{2} (1 + \varepsilon(v_{j-1}^n)^3)) v_{j+1}^{n+1} = (\mu - (1 - \theta) \frac{kh}{2} \\ (1 + \varepsilon(v_j^n)^3)) v_{j-1}^n - (2\mu + h^2) v_j^n + \\ (\mu + (1 - \theta) \frac{kh}{2} (1 + \varepsilon(v_j^n)^3)) v_{j+1}^n, \end{aligned} \quad (20)$$

so using Taylor's expansion, it can be shown that at point (x_j, t_n)

$$T_j^n = (v_t + (1 + \varepsilon v^3)v_x - \mu v_{xxt})_j^n + \frac{k}{2}(v_{tt} + 2\theta(1 + \varepsilon v^3)v_{xt})_j^n + \frac{h^2}{6}((1 + \varepsilon v^3)v_{xxx})_j^n, \quad (21)$$

but v is the solution of the differential equation, so

$$(v_t + (1 + \varepsilon v^3)v_x - \mu v_{xxt})_j^n = 0, \quad (22)$$

therefore, the principal part of local truncation error is

$$T_j^n = \frac{k}{2}(v_{tt} + 2\theta(1 + \varepsilon v^3)v_{xt})_j^n + \frac{h^2}{6}((1 + \varepsilon v^3)v_{xxx})_j^n, \quad (23)$$

hence the local truncation error is $O(h^2 + k)$.

4.2- First order, two level scheme (The 2nd scheme)- stability and error analysis

To apply the finite difference method for solving the GRLW equation, firstly we present the following notations for the derivatives

$$\begin{aligned} \frac{\partial u(x_j, t_n)}{\partial t} &\equiv (u_t)_j^n \cong \frac{u_j^{n+1} - u_j^n}{k}, \\ ((1 + \varepsilon v^p)u_x)_j^n &\cong \frac{1}{2}(1 + \varepsilon(u_{j-1}^n)^p) \frac{u_{j+1}^{n+1} - u_{j-1}^{n+1}}{2h} + \\ &\frac{1}{2}(1 + \varepsilon(u_j^n)^p) \frac{u_{j+1}^n - u_{j-1}^n}{2h}, \\ (u_{xxt})_j^n &\cong \frac{(u_{j+1}^{n+1} - 2u_j^{n+1} + u_{j-1}^{n+1}) - (u_{j+1}^n - 2u_j^n + u_{j-1}^n)}{kh^2}, \end{aligned} \quad (24)$$

where u_j^n is the exact solution at (x_j, t_n) , h and k are the spatial and temporal step sizes respectively and, $x_j = jh, t_n = nk$, $j = 0, 1, \dots$, and $n = 0, 1, \dots$, where superscript n denotes a quantity associated with time level t_n and subscript j denotes a quantity associated with space mesh point x_j . Now, we assume that u_j^n is the exact solution at the grid point (x_j, t_n) and U_j^n is the approximation solution at the same point. Then the finite difference scheme for (4) becomes,

$$\begin{aligned} \frac{U_j^{n+1} - U_j^n}{k} + \frac{1}{2}(1 + \varepsilon(U_{j-1}^n)^p) \frac{U_{j+1}^{n+1} - U_{j-1}^{n+1}}{2h} + \\ \frac{1}{2}(1 + \varepsilon(U_j^n)^p) \frac{U_{j+1}^n - U_{j-1}^n}{2h} - \\ \mu \frac{(U_{j+1}^{n+1} - 2U_j^{n+1} + U_{j-1}^{n+1}) - (U_{j+1}^n - 2U_j^n + U_{j-1}^n)}{kh^2} = 0, \end{aligned} \quad (25)$$

so,

$$\begin{aligned} (\mu + \frac{kh}{4}(1 + \varepsilon(U_{j-1}^n)^p))U_{j-1}^{n+1} - (2\mu + h^2)U_j^{n+1} + \\ (\mu - \frac{kh}{4}(1 + \varepsilon(U_{j-1}^n)^p))U_{j+1}^{n+1} = (\mu - \frac{kh}{4}(1 + \varepsilon(U_j^n)^p)) \\ U_{j-1}^n - (2\mu + h^2)U_j^n + (\mu + \frac{kh}{4}(1 + \varepsilon(U_j^n)^p))U_{j+1}^n, \end{aligned} \quad (26)$$

4.2.1. Stability of finite difference for (The 2nd scheme)

Lemma(2): The finite difference scheme (26) is a unconditional stable and if $u(x, t)$ is smooth enough, then the local truncation error T_j^n of the scheme (26) is $O(h + k)$.

Proof. Using Fourier method, assuming that u in the nonlinear term is locally constant. In case of applying the Von Neumann stability theory, the growth of Fourier mode takes the form

$$U_j^n = \zeta^n e^{ikx_j}, \quad (27)$$

where k is a mode number, h is the element size and $x_j = jh, i = \sqrt{-1}$,

now, substituting (27) into (26) yields

$$\begin{aligned} g[(\mu + Q)e^{-ikh} - (2\mu + h^2) + (\mu - Q)e^{ikh}] \\ = (\mu - Q)e^{-ikh} - (2\mu + h^2) + (\mu + Q)e^{ikh}, \end{aligned} \quad (28)$$

where $Q = \frac{kh}{4}(1 + \varepsilon(U_j^n)^p)$, $g = \frac{\zeta^{n+1}}{\zeta^n}$,

then we can get the amplification factor in the form

$$g = \frac{A + iB}{A - iB}, \quad (29)$$

where $A = 2\mu \cos kh - (2\mu + h^2)$, $B = 2Q \sin kh$.

Then we get

$$|g| = 1, \quad (30)$$

so we can say that The scheme is unconditional stable.

Now, to study the local truncation error of (26) we replace U_j^n by $v_j^n = u(x_j, t_n)$ represents the analytical solution for (4) with independent variables x and t and let $p = 3$, (GRLW) equation, then substituting it into (26) gives

$$\begin{aligned} (\mu + \frac{kh}{4}(1 + \varepsilon(v_{j-1}^n)^3))v_{j-1}^{n+1} - (2\mu + h^2)v_j^{n+1} + \\ (\mu - \frac{kh}{4}(1 + \varepsilon(v_{j-1}^n)^3))v_{j+1}^{n+1} = (\mu - \frac{kh}{4}(1 + \varepsilon(v_j^n)^3))v_{j-1}^n - \\ (2\mu + h^2)v_j^n + (\mu + \frac{kh}{4}(1 + \varepsilon(v_j^n)^3))v_{j+1}^n, \end{aligned} \quad (31)$$

so using Taylor's expansion, it can be shown that at point (x_j, t_n)

$$\begin{aligned} T_j^n = (v_t + (1 + \varepsilon v^3)v_x - \mu v_{xxt})_j^n + \frac{k}{2}(v_{tt} + \\ (1 + \varepsilon v^3)v_{xt} - h \frac{3\varepsilon}{2}(vv_x)^2)_j^n, \end{aligned} \quad (32)$$

but v is the solution of the differential equation, so

$$(v_t + (1 + \varepsilon v^3)v_x - \mu v_{xxt})_j^n = 0, \quad (33)$$

therefore, the principal part of local truncation error is

$$T_j^n = \frac{k}{2}(v_{tt} + (1 + \varepsilon v^3)v_{xt} - h \frac{3\varepsilon}{2}(vv_x)^2)_j^n, \quad (34)$$

hence the local truncation error is $O(h + k)$.

4.3- A Second Order, Three-Level scheme (The 3rd Scheme) - stability and error analysis

To apply the finite difference method for solving the GRLW equation, firstly we present the following notations for the derivatives

$$\frac{\partial u(x_j, t_n)}{\partial t} \equiv (u_t)_j^n \equiv \frac{u_j^{n+1} - u_j^{n-1}}{2k},$$

$$((1 + \varepsilon u^p)u_x)_j^n \equiv (1 + \varepsilon(u_j^n)^p) \frac{u_{j+1}^n - u_{j-1}^n}{2h}, \quad (35)$$

$$(u_{xxt})_j^n \equiv \frac{(u_{j+1}^{n+1} - 2u_j^{n+1} + u_{j-1}^{n+1}) - (u_{j+1}^{n-1} - 2u_j^{n-1} + u_{j-1}^{n-1})}{2kh^2},$$

where u^n is the exact solution at (x_j, t_n) and h, k are the spatial and temporal step sizes respectively and, $x_j = jh, t_n = nk, j = 0, 1, \dots$, and $n = 0, 1, \dots$, where superscript n denotes a quantity associated with time level t_n and subscript j denotes a quantity associated with space mesh point x_j . The scheme requires two initial time levels, so we use the analytical solution (6) at $t = 0$ and $t = k$.

Now, we assume that u_j^n is the exact solution at the grid point (x_j, t_n) and U_j^n is the approximation solution at the same point. Then the finite difference scheme for (4) becomes,

$$\begin{aligned} & \frac{U_j^{n+1} - U_j^{n-1}}{2k} + (1 + \varepsilon(U_j^n)^p) \frac{U_{j+1}^n - U_{j-1}^n}{2h} - \\ & \mu \frac{(U_{j+1}^{n+1} - 2U_j^{n+1} + U_{j-1}^{n+1}) - (U_{j+1}^{n-1} - 2U_j^{n-1} + U_{j-1}^{n-1})}{2kh^2} = 0, \end{aligned} \quad (36)$$

so, we can simplify as,

$$\begin{aligned} & \mu U_{j-1}^{n+1} - (2\mu + h^2)U_j^{n+1} + \mu U_{j+1}^{n+1} = \\ & -kh((1 + \varepsilon(U_j^n)^p))U_{j-1}^n + kh((1 + \varepsilon(U_j^n)^p))U_{j+1}^n + \\ & \mu U_{j-1}^{n-1} - (2\mu + h^2)U_j^{n-1} + \mu U_{j+1}^{n-1}, \end{aligned} \quad (37)$$

4.3.1- Stability of finite difference for (The 3rd Scheme)

Lemma(3): The finite difference scheme (37) is unconditional stable and if $u(x, t)$ is smooth enough, then the local truncation error T_j^n of the scheme (37) is $O(h^2 + k^2)$.

Proof. Using Fourier method, assuming that u in the nonlinear term is locally constant. In case of applying the Von Neumann stability theory, the growth of Fourier mode takes the form

$$U_j^n = \zeta^n e^{ikx_j}, \quad (38)$$

where k is a mode number, h is the element size and $x_j = jh, i = \sqrt{-1}$.

Now, substituting (38) into (37) yields

$$g^2 = \frac{\zeta^{n+1}}{\zeta^{n-1}}, \quad (39)$$

where g is the growth factor, and from (37) and (38) we get

$$g^2 - 2ig \sin \phi - 1 = 0, \quad (40)$$

where, $Q = kh(1 + \varepsilon(U_j^n)^p)$, $\sin \phi = \frac{Q \sin kh}{2\mu \cos kh - 2\mu - h^2}$, yields

$|g_1| = |g_2| = 1$, therefore the finite difference scheme is unconditional stable.

Now, to study the local truncation error of (37) we replace U_j^n by $v_j^n = u(x_j, t_n)$ represents the analytical solution for the Eq. (4) with independent variables x and t . and let $p = 3$, (GRLW) equation, then substituting it into (37) gives

$$\begin{aligned} & \mu v_{j-1}^{n+1} - (2\mu + h^2)v_j^{n+1} + \mu v_{j+1}^{n+1} = -kh((1 + \varepsilon(v_j^n)^3)) \\ & v_{j-1}^n + kh((1 + \varepsilon(v_j^n)^3))v_{j+1}^n + \mu v_{j-1}^{n-1} - \\ & (2\mu + h^2)v_j^{n-1} + \mu v_{j+1}^{n-1}, \end{aligned} \quad (41)$$

so using Taylor's expansion, it can be shown that at point (x_j, t_n)

$$\begin{aligned} T_j^n &= (v_t + (1 + \varepsilon v^3)v_x - \mu v_{xxt})_j^n + \frac{k^2}{6}(v_{ttt})_j^n + \\ & \frac{h^2}{6}((1 + \varepsilon v^3)v_{xxx})_j^n, \end{aligned} \quad (42)$$

but v is the solution of the differential equation, so

$$(v_t + (1 + \varepsilon v^3)v_x - \mu v_{xxt})_j^n = 0, \quad (43)$$

therefore, the principal part of local truncation error is

$$T_j^n = \frac{k^2}{6}(v_{ttt})_j^n + \frac{h^2}{6}((1 + \varepsilon v^3)v_{xxx})_j^n, \quad (44)$$

hence the local truncation error is $O(h^2 + k^2)$.

V. NUMERICAL TESTES AND RESULTS OF GRLW EQUATION

It has been shown in Section 2 that the GRLW equation has an analytical solution of the form (6). In this work, we consider $\mu = 1$ and present some numerical experiments to assign the numerical solution of single solitary wave, in addition to determine the solution of two and three soliton interactions at different time levels.

5.1- Single Solitary Waves

In previous section, we have provided three finite difference schemes for the GRLW equation, and we can take the following as an initial condition.

$$u(x, 0) = \sqrt{\frac{(p+2)c}{2p}} \operatorname{sech}\left(\frac{p}{2} \sqrt{\frac{c}{\mu(c+1)}}(x - x_0)\right), \quad (45)$$

The norms L_2 and L_∞ are used to compare the numerical results with the analytical values and the quantities I_1, I_2 and I_3 are shown to measure conservation for the schemes. Now, for comparison, we consider a test problem where, $p = 3, c = 0.1, \mu = 1, h = 0.1, x_0 = 40, \Delta t = k = 0.1$, with range $[0, 80]$. The simulations are done up to $t = 1$ and the value of θ in the first scheme is chosen to be 0.5. The invariants I_1, I_2 and I_3 are changed by less than 6.61×10^{-3} , 4.28×10^{-3} and 3.3147×10^{-4} , respectively in the computer program for the first scheme. And less than 6×10^{-4} , 3.9×10^{-4} and 2.982×10^{-5} , respectively for the second

scheme. The invariants I_1, I_2 and I_3 are approach to zero for third scheme. Errors, also, at time 1 are satisfactorily small L_2 -error = 2.0923×10^{-3} and L_∞ -error = 1.0287×10^{-3} for the first scheme, are satisfactorily small L_2 -error = 2.44805×10^{-4} and L_∞ -error = 1.56618×10^{-4} for the second scheme. And are satisfactorily small L_2 -error = 6.87621×10^{-5} and L_∞ -error = 3.87296×10^{-5} for third scheme. Our results are recorded in Table 1. These results illustrate that the third scheme has a highest accuracy and best conservation than other tow schemes. So we use it to study the motion of single solitary waves and interaction between two and three solitons.

Table 1 Invariants and errors for single solitary wave
 $p = 3, c = 0.1, h = 0.1, k = 0.1$ and $x_0 = 40, 0 \leq x \leq 80$

Schemes	t	I_1	I_2	I_3	L_2 -norm	L_∞ -norm
First scheme $\theta=0.5$	0.0	4.06257	1.13382	0.0929579	0.0	0.0
	0.2	4.06124	1.13296	0.0927818	4.17573E-4	1.93356E-4
	0.4	4.05992	1.13217	0.0926062	8.35398E-4	3.93477E-4
	0.6	4.0586	1.13124	0.0924311	1.25367E-3	5.99835E-4
	0.8	4.05727	1.13038	0.0922564	1.67257E-3	8.11744E-4
	1.0	4.05596	1.12953	0.0920823	2.09231E-3	1.02873E-3
Second scheme	0.0	4.06257	1.13382	0.0929512	0.0	0.0
	0.2	4.06245	1.13375	0.0929353	4.76782E-5	3.07749E-5
	0.4	4.06233	1.13367	0.0929195	9.59982E-5	6.18902E-5
	0.6	4.06221	1.13359	0.0929036	1.44961E-4	8.67077E-5
	0.8	4.06209	1.13351	0.0928878	1.94562E-4	1.24796E-4
	1.0	4.06197	1.13343	0.092872	2.44805E-4	1.56618E-4
Third scheme	0.0	4.06257	1.13382	0.0929506	0.0	0.0
	0.2	4.06257	1.13382	0.0929508	1.47337E-5	2.33635E-6
	0.4	4.06257	1.13382	0.0929511	2.89141E-5	1.80452E-5
	0.6	4.06257	1.13382	0.0929511	4.25705E-5	2.51291E-5
	0.8	4.06257	1.13382	0.0929511	5.58038E-5	3.21822E-5
	1.0	4.06257	1.13382	0.0929511	6.87621E-5	3.87296E-5

Now, we consider two different cases to study the motion of single soliton.

Case1. In this case we study the motion of single soliton by first, second scheme and third scheme. In this case, we choose $p = 3, c = 0.1, \mu = 1, h = 0.1, x_0 = 40, \Delta t = k = 0.1$ with range $[0, 80]$. The simulations are done up to $t = 5$. The invariants I_1, I_2 and I_3 are changed by less than 3.254×10^{-2} , 2.101×10^{-2} and 1.57323×10^{-3} percent, respectively for the first scheme. Errors, also, are satisfactorily small L_2 -error = 1.09547×10^{-2} and L_∞ -error = 6.07418×10^{-3} for the first scheme. And the invariants I_1, I_2 and I_3 are changed by less than 3.03×10^{-3} , 1.93×10^{-3} and 1.4403×10^{-4} , respectively for the second scheme. Errors, also, are satisfactorily small L_2 -error = 1.38547×10^{-3} and L_∞ -error = 8.223×10^{-4} , respectively for the second scheme. And the invariants I_1, I_2 and I_3 are approach to zero for third scheme. Errors, also, are satisfactorily small L_2 -error = 2.83131×10^{-4} and L_∞ -error = 1.55714×10^{-4} , respectively for third scheme. Our results are recorded in Table 2 and the motion of solitary wave is plotted at different time levels in Fig. 1.

Table 2 Invariants and errors for single solitary wave
 $c = 0.1, h = 0.1, k = 0.1$ and $x_0 = 40, 0 \leq x \leq 80$

Schemes	t	I_1	I_2	I_3	L_2 -norm	L_∞ -norm
First scheme $\theta=0.5$	0	4.06257	1.13382	0.0929579	0.0	0.0
	1	4.05596	1.12953	0.0920823	2.09231E-3	1.0287 E-3
	2	4.04939	1.12527	0.0912222	4.20985 E-3	1.25737 E-3
	3	4.04288	1.12107	0.0903721	6.37663 E-3	3.41835 E-3
	4	4.03642	1.11691	0.0895384	8.61725 E-3	1.71376 E-3
	5	4.03003	1.11281	0.088718	1.09547 E-2	6.07418 E-3
Second scheme	0	4.06257	1.13382	0.0929512	0.0	0.0
	1	4.06197	1.13343	0.0928721	2.44805E-4	1.56704 E-4
	2	4.06137	1.13305	0.0927931	5.05614E-4	3.17657 E-4
	3	4.06076	1.13266	0.0927144	7.82466E-4	4.82279 E-4
	4	4.06015	1.13228	0.0926356	1.07561E-3	6.50099 E-4
	5	4.05954	1.13189	0.0925565	1.38547E-3	8.22312 E-4
Third scheme	0	4.06257	1.13382	0.0929506	0.0	0.0
	1	4.06257	1.13382	0.0929511	6.87621E-5	3.87296E-5
	2	4.06256	1.13382	0.0929497	1.33612E-4	6.69156E-5
	3	4.06255	1.13382	0.0929495	1.95752E-4	1.23942E-4
	4	4.06254	1.13382	0.0929542	2.44621E-4	1.43124E-4
	5	4.06252	1.13382	0.0929505	2.83131E-4	1.55714E-4

The motion of solitary wave using third scheme is plotted at times $t = 0, t = 5$ in Fig. 1

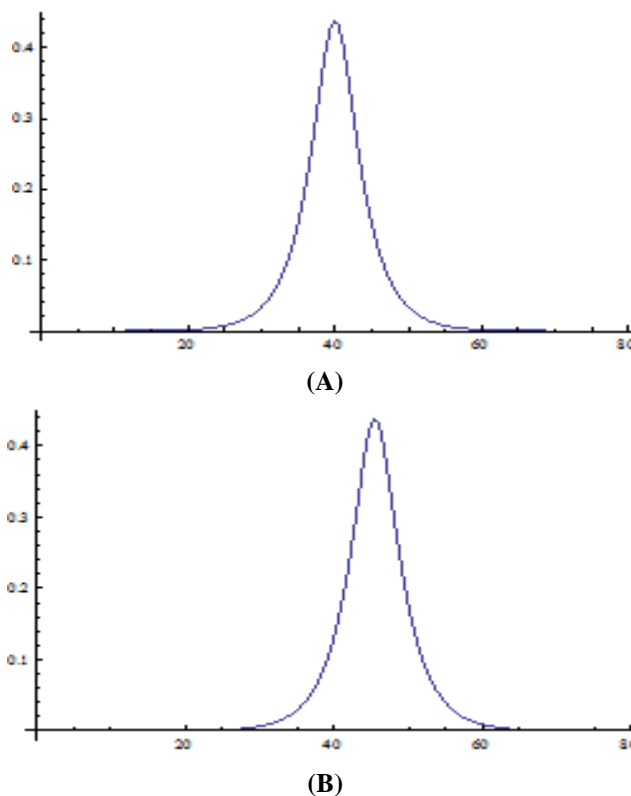


Fig. 1 Single solitary wave with $c = 0.1, h = 0.1, k = 0.1$ and $x_0 = 40, 0 \leq x \leq 80, t = 0, t = 5$

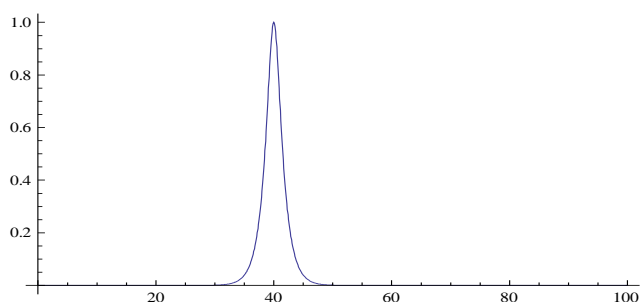
Case 2. In this case we study the motion of single soliton by third scheme. In this case, we choose $p = 3, c = 1.2, \mu = 1, h = 0.1, x_0 = 40, \Delta t = k = 0.025$ with range $[0, 100]$. The simulations are done up to $t = 2.5$. The invariants I_1 and I_2 approach to zero and I_3 is changed by less than 3.34×10^{-5} percent, respectively. Errors, also, are satisfactorily small L_2 -error = 6.71998×10^{-3} and L_∞ -error =

4.13724×10^{-3} , percent, respectively. Our results are recorded in Table 3 and the motion of solitary wave is plotted at different time levels in Fig. 2.

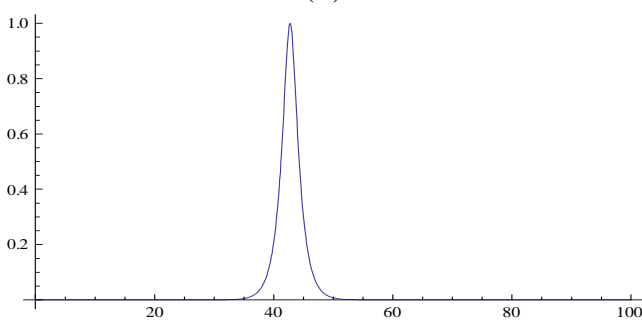
Table 3 Invariants and errors for single solitary wave
 $c = 1.2, h = 0.1, k = 0.025$ and $x_0 = 40, 0 \leq x \leq 100$

t	I ₁	I ₂	I ₃	L ₂ -norm	L _∞ -norm
0.0	3.79713	2.87871	0.975451	0.0	0.0
1.0	3.79714	2.87872	0.975109	2.73921E-3	1.06731E-3
1.5	3.79714	2.87872	0.975077	4.04478E-3	1.92657E-3
2.0	3.79714	2.87872	0.975096	5.37684E-3	3.36847E-3
2.5	3.79713	2.87872	0.975117	6.71998E-3	4.13724E-3

The motion of solitary wave using third scheme is plotted at times $t = 0, t = 2$ in Fig. 2



(A)



(B)

Fig. 2 Single solitary wave with $c = 1.2, h = 0.1, k = 0.025$ and $x_0 = 40, 0 \leq x \leq 100, t = 0, t = 2$

In the next table we make comparison between the results of third scheme and the results have been published in Search [25].

Table 4 Invariants and errors for single solitary wave
 $c = 1.2, h = 0.1, k = 0.025$ and $x_0 = 40, 0 \leq x \leq 100, \text{Time}=2$

Method	I ₁	I ₂	I ₃	L ₂ -norm	L _∞ -norm
Analytical	3.79713	2.87871	0.975451	0.0	0.0
Our scheme	3.79713	2.87872	0.975096	5.37684E-3	3.36847E-3
[25]	3.79713	2.88122	0.972388	2.13434E-3	1.47042E-3

The results of two numerical methods and the analytical schemes are similar.

5.2- Interaction of two solitary waves:

The interaction of two GRLW solitary waves having different amplitudes and traveling in the same direction is illustrated. We consider GRLW equation with initial conditions given by the linear sum of two well separated solitary waves of various amplitudes

$$u(x,0) = p \sqrt{\frac{(p+2)c_i}{2p} \operatorname{sech}\left(\frac{p}{2} \sqrt{\frac{c_i}{\mu(c_i+1)}}(x-x_i)\right)}, \quad (46)$$

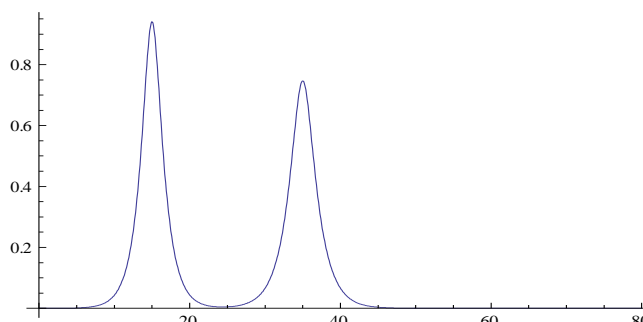
where, $i = 1, 2, x_i$ and c_i are arbitrary constants. In our computational work, we choose $c_1 = 1, c_2 = 0.5, x_1 = 15, x_2 = 35, \mu = 1, h = 0.1, k = 0.1$ with interval $[0, 80]$. In Fig.3 the interactions of these solitary waves are plotted at different time levels. We also, observe an appearance of a tail of small amplitude after interaction and the three invariants for this case are shown in Table 5. The invariants I_1, I_2 and I_3 are changed by less than $3.65 \times 10^{-3}, 1.06 \times 10^{-3}$ and 9.51×10^{-3} percent, respectively for the third scheme.

Table 5 Invariants of interaction two solitary waves of GRLW equation (third scheme)

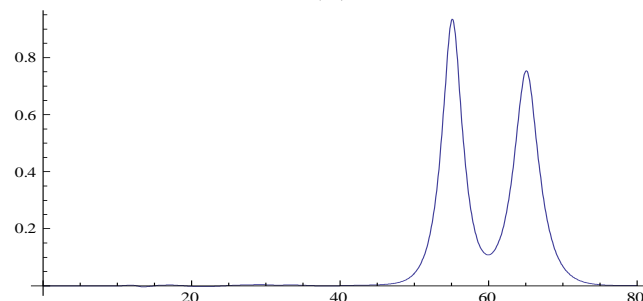
$c_1 = 1, c_2 = 0.5, x_1 = 15, x_2 = 35, 0 \leq x \leq 80$

t	I ₁	I ₂	I ₃
0	7.35999	4.51982	1.15572
2	7.36009	4.52078	1.15111
4	7.36001	4.52081	1.15022
6	7.35984	4.52081	1.15008
8	7.35984	4.52007	1.15005
10	7.35925	4.52061	1.15084
12	7.35925	4.52046	1.15243
14	7.35835	4.52035	1.15333
16	7.35783	4.52008	1.15514
18	7.35721	4.51958	1.15875
20	7.35634	4.51876	1.16523

The motion of interaction two solitary waves using third scheme is plotted at times $t = 0, t = 20$ in Fig.3



(A)



(B)

Fig. 3 interaction two solitary waves with $c_1 = 1, c_2 = 0.5, x_1 = 15, x_2 = 35, 0 \leq x \leq 80, t = 0, t = 20$

5.3 -Interaction of three solitary waves:

The interaction of three GRLW solitary waves having different amplitudes and traveling in the same direction is illustrated. We consider the GRLW equation with initial conditions given by the linear sum of three well separated solitary waves of various amplitudes:

$$u(x,0) = p \sqrt{\frac{(p+2)c_i}{2p} \operatorname{sech}\left(\frac{p}{2} \sqrt{\frac{c}{\mu(c+1)}}(x-x_i)\right)} \quad (47)$$

where, $i=1,2,3$, x_i and c_i are arbitrary constants. In our computational work, we choose $c_1=1, c_2=0.75, c_3=0.5$, $x_1=15, x_2=35, x_3=45$ with interval $[0, 80]$. In Fig. 4 the interactions of these solitary waves are plotted at different time levels. We also, observe an appearance of a tail of small amplitude after interaction and the three invariants for this case are shown in Table 6. The invariants I_1, I_2 and I_3 are changed by less than 3.492×10^{-1} , 7.392×10^{-2} and 9.45×10^{-2} percent, respectively for the third scheme.

Table 6 Invariants of interaction three solitary waves of GRLW equation (third scheme)

$c_1=1, c_2=0.75, c_3=0.5, x_1=15, x_2=35, x_3=45, 0 \leq x \leq 80$

t	I_1	I_2	I_3
0	11.0225	6.85174	1.77286
2	11.0226	6.85291	1.77266
4	11.0225	6.85204	1.77982
6	11.0222	6.85211	1.78224
8	11.0222	6.85239	1.78509
10	11.0216	6.85238	1.78618
12	11.0211	6.85173	1.78709
14	11.0201	6.85202	1.78455
16	11.0157	6.85218	1.78203
18	10.9834	6.85203	1.77842
20	10.6733	6.77782	1.86736

The motion of interaction three solitary waves using third scheme is plotted at times $t=0, t=15$ in Fig.4

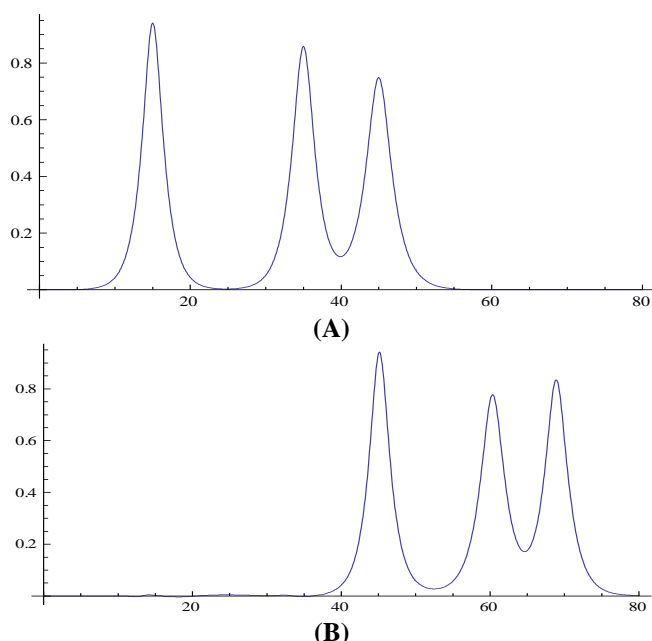


Fig. 4 Interaction three solitary waves with

$c_1=1, c_2=0.75, c_3=0.5, x_1=15, x_2=35,$

$x_3=45, 0 \leq x \leq 80, t=0, t=15$

5.4 -The Maxwellian Initial Condition

In final series of numerical experiments, the development of the Maxwellian initial condition

$$u(x,0) = \exp(-(x-40)^2) \quad (48)$$

into a train of solitary waves is examined. We apply it to the problem for different cases:

(I) $\mu=0.1$, (II) $\mu=0.05$, (III) $\mu=0.04$ and (IV) $\mu=0.015$, (V) $\mu=0.01$. When μ is large such as case (I), only single soliton is generated as shown in Fig.5, but the initial pulse developed to a rapidly oscillating wave packet as shown in Fig. 5a. However, when μ is reduced, more and more solitary waves are formed, since for case (II), two solitary waves is generated as shown in Fig. 5b, and for case (III) the Maxwellian pulse breaks up into a train of at least two solitary waves as shown in Fig. 6a. Finally, for (IV) and (V) cases, the Maxwellian initial condition has decayed into three stable solitary waves as shown in Fig. 6b and Fig. 7. The peaks of the well-developed wave lie on a straight line so that their velocities are linearly dependent on their amplitudes and we observe a small oscillating tail appearing behind the last wave as shown in the figures 5, 6 and 7, and all states at $t=5$. Moreover, the total number of solitary waves which are generated from the Maxwellian initial condition according to the results obtained from the numerical scheme in test problem as shown in Table 8, can be shown to follow approximately the relation

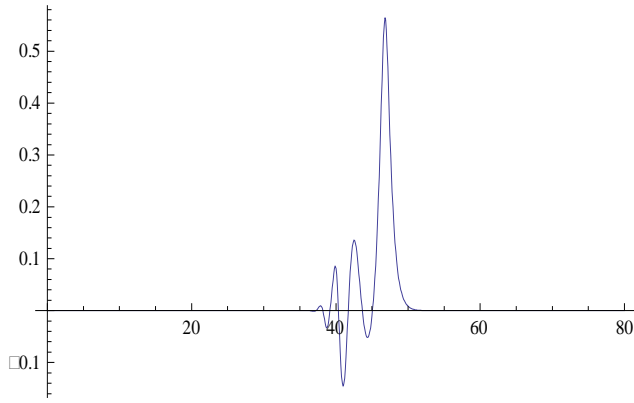
$$N \cong \left\lceil \frac{1}{\sqrt[4]{\mu}} \right\rceil, \quad (49)$$

Table 7 The values of the quantities I_1, I_2 and I_3 for the cases: $\mu=0.1, \mu=0.05, \mu=0.04, \mu=0.015$ and $\mu=0.01$

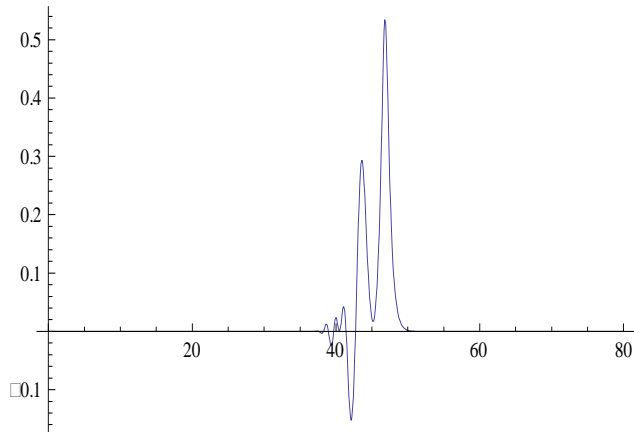
μ	t	I_1	I_2	I_3
0.1	3	1.09832	0.504005	0.0413785
	4	1.07554	0.483843	0.0335612
	5	1.05999	0.470552	0.0285704
0.05	3	1.08669	0.425156	0.0341883
	4	1.06887	0.409772	0.0274456
	5	1.05628	0.399312	0.0230417
0.04	3	1.08751	0.414439	0.0361086
	4	1.07094	0.400416	0.0297747
	5	1.05901	0.390753	0.0254186
0.015	3	1.06049	0.370616	0.0433279
	4	1.03577	0.351375	0.0361025
	5	1.01765	0.337731	0.0310671
0.01	3	1.04404	0.352908	0.0426219
	4	1.01932	0.333505	0.0354171
	5	1.00134	0.319882	0.0303963

Table 8 Solitary Waves Generated from a Maxwellian Initial Condition

μ	Number of solitary waves
0.1	1
0.05	2
0.04	2
0.015	3
0.01	3

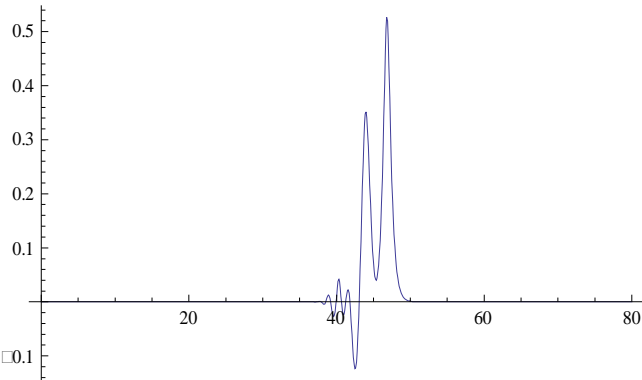


(A)

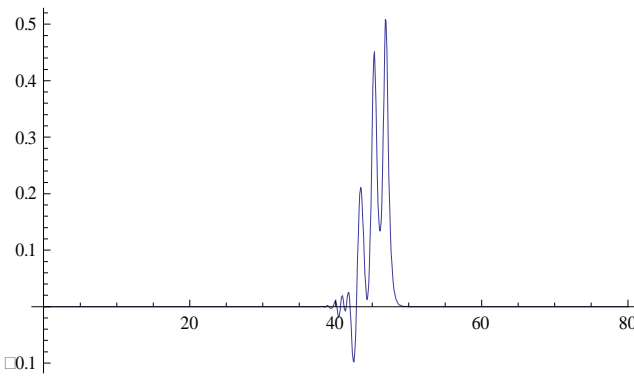


(B)

Fig. 5 The Maxwellian initial condition at (I) $\mu = 0.1$, (II) $\mu = 0.05$, and $t = 5$



(A)



(B)

Fig. 6 The Maxwellian initial condition at (III) $\mu = 0.04$, (IV) $\mu = 0.015$, and $t = 5$

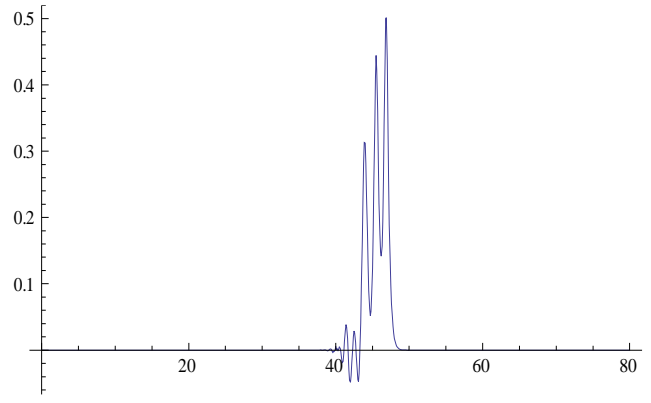


Fig. 7 The Maxwellian initial condition at (V) $\mu = 0.01$, and $t = 5$

VI. CONCLUSIONS

In this paper, we have applied a finite difference method to study solitary waves, and show that the scheme is unconditional stable. We tested our scheme through a single solitary wave in which the analytic solution is known and then extend it to study the interaction of solitons where no analytic solution is known during the interaction. The Maxwellian initial condition has been used and a relation between μ and the number of waves was explored. Moreover, despite the fact that the wave does not change, results show that the interaction results atail of small amplitude in two and clearly three soliton interactions, and the conservation laws were satisfactorily satisfied. The appearance of such tail can be beneficial in further study.

REFERENCES

- [1] D. H. Peregrine (1966), Calculations of the development of an undular bore, *J. Fluid Mech.* vol. 25 (2) , pp. 321–330.
- [2] J. C. Eilbeck, G.R. McGuire (1975), Numerical study of regularized long wave equation, I: numerical methods, *J. Comput. Phys.* vol. 19, pp. 43–57.
- [3] J. L. Bona, P.J. Pyrant (1973), A mathematical model for long wave generated by wave makers in nonlinear dispersive systems, *Proc. Comp. Philos. Soc.* vol. 37 , pp. 391.
- [4] J. L. Bona, W.G. Pritchard, L.R. Scott (1985), Numerical scheme for a model of nonlinear dispersive waves, *J. Comput. Phys.* vol. 60, pp. 167– 176.
- [5] M.E. Alexander, J.H. Morris (1979), Galerkin method for some model equation for nonlinear dispersive waves, *J. Comput. Phys.* vol.30, pp. 428–451.
- [6] D. J. Evans, K.R. Raslan (2005), The Tanh function method for solving some important nonlinear partial differential equations, *Int. J. comput. Math.* vol. 82 (7), pp. 897–905
- [7] P. C. Jain, R. Shankar, T.V. Single (1993), Numerical solutions of RLW equation, *Commun. Numer. Meth. Eng.* vol. 9, pp. 587–594.
- [8] D. Bhardwaj, R. Shankar (2000), A computational method for regularized long wave equation, *Comput. Math. Appl.* vol. 40, pp. 1397–1404.
- [9] S.I. Zaki (2001), Solitary waves of the spitted RLW equation, *Comput. Phys. Commun.* vol. 138, pp. 80–91.
- [10] L. R. T. Gardner, G.A. Gardner, A. Dogan (1996), A least squares finite element scheme for the RLW equation, *Commun. Numer. Meth. Eng.* vol. 12, pp. 795–804.
- [11] I. Dag (2000), Least squares quadratic B-splines finite element method for the regularized long wave equation, *Comput. Meth. Appl. Mech. Eng.* vol. 182, pp. 205–215.
- [12] A. A. Soliman, K.R. Raslan (2001), Collocation method using quadratic B-spline for the RLW equation. *Int. J. Comput. Math.* vol. 78, pp. 399–412.
- [13] I. Dag, B. Saka, D. Irk (2004), Application of cubic B-splins for numerical solution of the RLW equation, *Appl. Math Comput.* vol. 195, pp. 373–389.

- [14] K. R. Raslan (2005), A computational method for the regularized long wave (RLW) equation, Appl. Math. Comput. vol. 176, pp. 1101–1118.
- [15] A.A. Soliman, M.H. Hussien (2005), Collocation solution for RLW equation with septic splines, Appl. Math. Comput. vol. 161, pp. 623–636.
- [16] L. R .T. Gardner, G.A. Gardner, F.A. Ayoub, N.K. Amein (1997), Approximations of solitary waves of the MRLW equation by B-spline finite element, Arab. J. Sci. Eng. Vol. 22, pp. 183–193.
- [17] A. K. Khalifa, K.R. Raslan, H.M. Alzubaidi, (2007), A finite difference scheme for the MRLW and solitary wave interactions Applied Mathematics and Computation, vol. 189, pp. 346–354.
- [18] K. R. Raslan, S. M. Hassan (2009), Solitary waves for the MRLW equation, Applied Mathematics Letters, vol. 22 , pp. 984-989.
- [19] A. K. Khalifa, K. R. Raslan, H. M. Alzubaidi(2007), A collocation method with cubic B- splines for solving the MRLW equation, Comput. Appl. Math. vol. 212, pp. 406- 418.
- [20] Saleh M .Hassan,D.G.Alamery (2009), B-splines Collocation Algorithms for Solving Numerically the MRLW Equation ,international Journal of Nonlinear Science. vol. 8(2), pp. 131-140.
- [21] Mokhtari, R., Mohammadi, M. (2010), Numerical solution of GRLW equation using Sinc- collocation method. Comput. Phys. Commun. vol. 181, pp. 1266-1274.
- [22] D. Kaya (2004), A numerical simulation of solitary wave solutions of the generalized regularized long wave equation, Appl. Math.Comput. vol. 149, pp. 833–841.
- [23] Talaat S. El-Danaf, Mohamed A. Ramadan and Faysal E.I. Abd Alaal (2005), The use of adomian decomposition method for solving the regularized long-wave equation , Chaos, Solitons & Fractals. vol. 26(3), pp. 747-757.
- [24] P.J. Olver (1979), Euler operators and conservation laws of the BBM equation, Math. Proc. Comb. Phil. Soc. vol. 85 , pp. 143-159.
- [25] Thoudam Roshan, (2012), A petrov-Galerkin method for solving the generalized regularized long wave (GRLW) equation,Appl.Math.Comput.vol. 63, pp. 943-956.
- [26] Mohammadi, M., Mokhtari, R. (2011), Solving the generalized regularized long wave equation on the basis of a reproducing kernel space. J. Comput. Appl. Math.vol. 235, pp. 4003–4014 .



Talaat S. EL-Danaf, Mathematics Department, Faculty of Science, Al-Azhar University, Nasr-City, Cairo.